JOURNAL OF COMPUTATIONAL PHYSICS 99, 203–208 (1992)

The Inclusion of Collisional Effects in the Splitting Scheme

L. DEMEIO*

Center for Transport Theory and Mathematical Physics, Virginia Polytechnic Institute and State University, Blacksburg, Virginia 24061

Received July 13, 1990; revised February 15, 1991

An algorithm is given for the numerical solution of the Boltzmann equation for a one-dimensional unmagnetized plasma with immobile ions, in which collisional effects are described by the Bhatnagar–Gross–Krook (BGK) model. The algorithm is a straightforward generalization of the splitting scheme, which solves the one-dimensional Vlasov–Poisson system. The accuracy of the splitting scheme to second order in Δt is preserved.

1. INTRODUCTION

Considerable progress has been made in the last ten years in understanding the nonlinear evolution of stable and unstable plasma waves [1–5] thanks to the appearance of the splitting scheme algorithm [1], which solves the Vlasov–Poisson system (VP) for a one-dimensional unmagnetized collisionless plasma with fixed ions

$$\frac{\partial f}{\partial t}+v\frac{\partial f}{\partial x}-E\frac{\partial f}{\partial v}=0 \tag{1}$$

$$\frac{\partial E}{\partial x}=1-\int f\,dv. \tag{2}$$

Here, $x\in[0, L]$, $v\in(-\infty,\infty)$ and $t\in[0,\infty)$ are the space, velocity, and time variable (measured in units of the Debye length, the thermal velocity, and the plasma period, respectively); $E=E(x,t)$ is the self-consistent electric field and $f=f(x,v,t)$, the electron distribution.

Besides some analytical results concerning the full nonlinear collisionless problem [6, 7], models have been developed (see [8, 9] and references cited therein) in which a small collisional term is included in Eq. (1) in the Bhatnagar–Gross–Krook (BGK) form [10, 11]; in particular, interesting predictions have been made about the saturation of weakly unstable modes with possible appearance of double frequency behaviour [8, 9]. Some numerical calculations have been performed for the BGK model in the case of a neutral gas by means of finite difference techniques [12, 13].

With the BGK collision operator, Eq. (1) becomes

$$\frac{\partial f}{\partial t}+v\frac{\partial f}{\partial x}-E\frac{\partial f}{\partial v}=\nu(f_{\mathrm{eq}}-f), \tag{1a}$$

with ν the (dimensionless) collision frequency and f_{eq} the local Maxwellian; i.e.,

$$f_{\mathrm{eq}}(x,v,t)=\rho(x,t)\,M(v), \tag{3}$$

with $\rho(x,t)=\int f\,dv$ and $M(v)=\exp(-v^2/2)/\sqrt{2\pi}$. Equations (1a)–(2) are to be solved subject to the initial condition $f(x,v,0)\equiv g(x,v)$; moreover, we impose periodic boundary conditions, i.e., $f(0,v,t)=f(L,v,t)$ and $E(0,t)=E(L,t)$.

In this work, we show how the BGK model can be incorporated in the splitting scheme and produce a few examples showing the effect of collisions on linearly stable (Landau damping) and unstable distributions. As far as the numerical verification of the theory developed in [8, 9] is concerned, we have not been able to observe the kind of behaviour predicted there, but this is probably due to the difficulty in preparing the initial data according to the given prescription, which requires a good deal of separate numerical work.

2. THE METHOD

The Vlasov–Poisson system (1)–(2) is equivalent to the characteristic system

$$\dot{x}=v \tag{4}$$

$$\dot{v}=-E(x,t) \tag{5}$$

* Present address: Chemistry Dept., University of British Columbia, 2036 Main Mall, Vancouver, BC, Canada V6T 1Y6.

0021-9991/92 $3.00

(with $\partial E/\partial x = 1 - \int f\,dv$). The distribution function is constant along the characteristic lines given by the solution of (4)–(5), so that its value at the time t on the point (x, v) of the phase space can be found by tracing back to $t = 0$ the characteristic line passing by (x, t) at time t.

For the numerical solution the phase space has to be discretized and a cutoff V has to be introduced in the velocity variable. Let $\{x_i, v_j\}$, $i = 1, N+1; j = 1, M$ be the discretized phase space, with $x_1 = 0$, $x_N = L$, $v_1 = -V$, $v_M = V$, $x_{i+1} = x_i + \Delta x$, $v_{j+1} = v_j + \Delta v$, $\Delta x = L/(N-1)$, and $\Delta v = 2V/(M-1)$. At each time t, the $M \times (N+1)$ values for the distribution function at each mesh point, $f(x_i, v_j, t) = f_{ij}(t)$, $i = 1, N+1; j = 1, M$, have to be calculated, with the boundary conditions

$$f_{Nj}(t) = f_{1j}(t), \qquad j = 1, M$$
$$f_{N+1,j}(t) = f_{2j}(t), \qquad j = 1, M$$
$$f_{iM}(t) = f_{i1}(t) = 0, \qquad i = 1, N+1.$$

The splitting scheme performs the integration of (VP) along the characteristics using interpolation methods. Suppose that the values of f at the time $t - \Delta t$ on the mesh points, $f_{ij}(t - \Delta t)$, $i = 1, N+1$, $j = 1, M$, are known. Let us define, for convenience, $x_{ij}(t - \Delta t)$ and $v_{ij}(t - \Delta t)$ as the solution of the characteristic system (4)–(5) corresponding to the boundary conditions $x(t) = x_i$ and $v(t) = v_j$. Then, the values of f at the time t on the mesh points coincide with the values of f at the time $t - \Delta t$ on the off-mesh points $(x_{ij}(t - \Delta t), v_{ij}(t - \Delta t))$: $f_{ij}(t) = f(x_{ij}(t - \Delta t), v_{ij}(t - \Delta t), t - \Delta t)$. These values of f are interpolated from the $f_{ij}(t - \Delta t)$; in our code the interpolation is performed by using cubic splines (an alternate version of the algorithm exists, which uses fast Fourier transforms to operate the interpolation [14]). It has been shown that this scheme gives the solution correct to second order in Δt. In particular, the integrated equations for the characteristics give [1]

$$x_{ij}(t - \Delta t) = x_i - v_j\,\Delta t - \tfrac{1}{2}\bar{E}_i\,\Delta t^2 + \mathcal{O}(\Delta t^3) \tag{6}$$

$$v_{ij}(t - \Delta t) = v_j + \bar{E}_i\,\Delta t + \mathcal{O}(\Delta t^3), \tag{7}$$

where $\bar{E}_i$ is the value of the electric field at $t + \Delta t/2$ (see [1] for details).

The integration over v, which gives the density, can be expressed as

$$\rho(x_i, t) \equiv \rho_i(t) = \sum_{j=1}^{M} w_j f_{ij}, \tag{8}$$

where the w_j's, $j = 1, M$, are the weights, which depend on the integration scheme used. For example, in our code (which we have implemented on the Cray Y-MP of the Pittsburgh Supercomputing Center, see [15]) we have used Simpson's $\frac{3}{8}$ rule, for which the weights are

$$w_j = \begin{cases} 3\,\Delta v/8, & j = 1 \text{ and } M \\ 6\,\Delta v/8, & j = 4, 7, 10, ..., M-3 \\ 9\,\Delta v/8, & \text{otherwise.} \end{cases}$$

The integration over x, which gives the electric field is performed by using Fourier transforms.

In the presence of collisions, $f(x, v, t)$ is no longer constant along the Vlasov characteristics, since instead of $df/dt = 0$ we now have $df/dt = -\nu(f - f_{\text{eq}})$, so the idea for producing numerical solutions of (1a)–(2) is to account for the variation of f along the Vlasov characteristics at each time step. We now have

$$\begin{aligned} f(x(t), v(t), t) &= f(x(t - \Delta t), v(t - \Delta t), t - \Delta t) \\ &\quad - \nu \int_{t-\Delta t}^{t} dt'\,[f(x(t'), v(t'), t') \\ &\quad - \rho(x(t'), t')\,M(v(t'))] \end{aligned} \tag{9}$$

which, after using the trapezoidal rule, becomes

$$\begin{aligned} f(x(t), v(t), t) &= f(x(t - \Delta t), v(t - \Delta t), t - \Delta t) \\ &\quad - \nu \frac{\Delta t}{2}\,[f(x(t), v(t), t) \\ &\quad + f(x(t - \Delta t), v(t - \Delta t), t - \Delta t) \\ &\quad - \rho(x(t), t)\,M(v) \\ &\quad - \rho(x(t - \Delta t), t - \Delta t)\,M(v(t - \Delta t))] \end{aligned}$$

and

$$\begin{aligned} f(x(t), v(t), t)\left(1 + \frac{\nu\,\Delta t}{2}\right) &= f(x(t - \Delta t), v(t - \Delta t), t - \Delta t) \\ &\quad \times \left(1 - \frac{\nu\,\Delta t}{2}\right) + \frac{\nu\,\Delta t}{2}\,[\rho(x(t), t)\,M(v) \\ &\quad + \rho(x(t - \Delta t), t - \Delta t)\,M(v(t - \Delta t))], \end{aligned} \tag{10}$$

where $f(x(t), v(t), t)$ is the unknown value of the distribution function at the mesh point $x(t) = x$, $v(t) = v$, and $f(x(t - \Delta t), v(t - \Delta t), t - \Delta t)$ is the value of the distribution along the Vlasov characteristic at the time $t - \Delta t$ and which is calculated by the splitting scheme in the way described above. In an analogue way, the values $\rho(x(t - \Delta t), t - \Delta t)$ are interpolated from the known $\rho_i(t - \Delta t)$ using (6). Note that, although ρ is a function of x and t only,

$\rho(x(t-\Delta t), t-\Delta t)$ depends on v via $x(t-\Delta t)$. With the same understanding, $M(v(t-\Delta t))$, which is calculated using (7), depends on x.

With the definitions

$$f_{ij}^{(0)} = f(x_{ij}(t-\Delta t), v_{ij}(t-\Delta t), t-\Delta t)$$
$$\rho_{ij}^{(0)} = \rho(x_{ij}(t-\Delta t), t-\Delta t)$$
$$M_j = M(v_j)$$
$$M_{ij}^{(0)} = M(v_{ij}(t-\Delta t)),$$

the discretized version of (10) becomes

$$f_{ij}\left(1+\frac{\nu\,\Delta t}{2}\right) = f_{ij}^{(0)}\left(1-\frac{\nu\,\Delta t}{2}\right) + \frac{\nu\,\Delta t}{2}\left[\rho_i M_j + \rho_{ij}^{(0)} M_{ij}^{(0)}\right].$$

By using (8) we then have

$$f_{ij}\left(1+\frac{\nu\,\Delta t}{2}\right) = f_{ij}^{(0)}\left(1-\frac{\nu\,\Delta t}{2}\right) + \frac{\nu\,\Delta t}{2}\left(\sum_{l=1}^{M} w_l f_{il} M_j + \rho_{ij}^{(0)} M_{ij}^{(0)}\right),$$

which, after some straightforward algebra, can be put in the matrix form

$$F \times \Lambda = \Theta, \tag{11}$$

with F, Λ, and Θ the matrices whose elements are given by

$$F_{ij} = f_{ij}, \qquad i = 1, N+1; \quad j = 1, M$$
$$\Lambda_{ij} = \delta_{ij} - \frac{\nu\,\Delta t/2}{1+\nu\,\Delta t/2} w_i M_j, \qquad i, j = 1, M;$$
$$\Theta_{ij} = \frac{1-\nu\,\Delta t/2}{1+\nu\,\Delta t/2} f_{ij}^{(0)} + \frac{\nu\,\Delta t/2}{1+\nu\,\Delta t/2} \rho_{ij}^{(0)} M_{ij}^{(0)},$$
$$i = 1, N+1; \quad j = 1, M$$

(repeated indices are not summed over). Finally, $F = \Theta \times \Lambda^{-1}$ solves for the distribution funcion on the mesh points at time t. The inversion of Λ does not pose any problem, since (for $\nu \leqslant 1$) it is close to the unit matrix.

In carrying out this procedure, the splitting scheme is used, first, to find $f_{ij}^{(0)}$ and $\rho_{ij}^{(0)}$ by interpolation; then, the matrix Θ can be constructed and the new values of f can be found upon multiplication by the inverse of Λ.

The inclusion of collisional effects makes the code slower by a factor ≈ 2.5, mainly because of the two new one-dimensional interpolations needed to calculate $\rho(x(t-\Delta t), t-\Delta t)$ and $M(v(t-\Delta t))$. However, since collisions virtually remove the filamentation problem [1, 16], fewer mesh points are needed in the velocity variable in most cases.

Note that Eq. (9) is formally correct for any ν. However, a highly collisional plasma, say $\nu > 1$, does not evolve along the Vlasov characteristics and the use of this method would become impractical, because an unrealistically small time step Δt would have to be used. Therefore, we anticipate that the present algorithm can be effectively used for $\nu \leqslant 1$. The use of the trapezoidal rule is consistent with the accuracy of the splitting scheme, since the error induced in calculating the integral on the r.h.s. of (9) is of the order of $(\Delta t)^3$.

3. EXAMPLES

a. *Relaxation of a Spatially Uniform Distribution*

When the initial condition $g(x, v)$ is any spatially homogeneous distribution, say $g(x, v) = f_0(v)$, the solution of (1a)–(2) is known [10, 11],

$$f(x, v, t) = M(v) + (f_0(v) - M(v))\, e^{-\nu t}, \tag{12}$$

showing that the system relaxes towards the thermal equilibrium with a characteristic time ν^{-1}. No spatial dependence develops and $E(x, t) \equiv 0$ for all t.

This serves as a first check of our numerical scheme. We choose a symmetric bump-on-tail initial distribution, namely,

$$f_0(v) = \frac{1}{\sqrt{2\pi}} n_p e^{-v^2/2} + n_b\left[\frac{1}{\sqrt{2\pi}} e^{-((v-V_0)/v_t)^2/2} + \frac{1}{\sqrt{2\pi}} e^{-((v+V_0)/v_t)^2/2}\right], \tag{13}$$

with $n_p = 0.9$, $n_b = 0.1$, $V_0 = 4.5$, and $v_t = 0.5$. In our simulation, which we ran up to 50 plasma periods, the electric field was identically zero for all t, while the distribution function remained spatially uniform with a time dependance in perfect agreement with (12), as can be seen from Fig. 1, where f is shown as a function of v at selected times in the region of the bump at positive velocities.

b. *Effect of Collisions on Landau Damping*

As is well known from the solution of the linearized Vlasov–Poisson system [17, 18], when the initial distribution is chosen near a spatially uniform Maxwellian, with the further requirement that it be the restriction to the real axis of a function analytic in the complex v plane, the electric field decreases exponentially in time, its kth Fourier transform exhibiting damped oscillations at a frequency ω and a

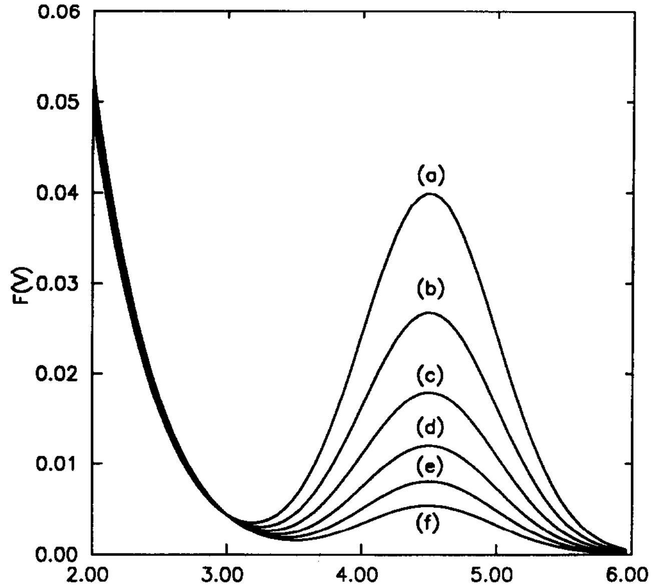

FIG. 1. Distribution function for the case of Example a at $t=0$ (a); $t=10$ (b); $t=20$ (c); $t=30$ (d); $t=40$ (e); $t=50$ (f).

damping rate γ given by the roots of the Landau dispersion relation [17],

$$\Lambda_k(z) \equiv 1 - \frac{1}{k^2} \int_{\mathscr{L}} \frac{\partial f_0/\partial v}{v-z}\, dv = 0, \tag{14}$$

where $z=(\omega+i\gamma)/k$, $\mathscr{L}$ is the well known Landau contour and $f_0 = M(v)$ in this case. Using the *plasma dispersion function* [19], defined for $\operatorname{Im} z > 0$ as

$$Z(z) \equiv \frac{1}{\sqrt{\pi}} \int_{-\infty}^{+\infty} \frac{e^{-x^2}}{x-z}\, dx,$$

and by analytic continuation for $\operatorname{Im} z \leqslant 0$, Eq. (14) can be written as

$$1+\frac{1}{k^2}\left[1+\frac{z}{\sqrt{2}} Z\left(\frac{z}{\sqrt{2}}\right)\right]=0. \tag{15}$$

TABLE I

Solution of the Dispersion Relation for the Maxwellian Case with $k=0.5$

ν	ω	γ
0.0	1.42	−0.15
0.01	1.42	−0.16
0.05	1.42	−0.20
0.1	1.42	−0.25

In the presence of collisions, described by the BGK model, it is easily seen that the dispersion relation becomes [10, 11]

$$1 - \frac{1}{k^2} \int_{\mathscr{L}} \frac{\partial f_0/\partial v - iMvk}{v - z - i\nu/k}\, dv = 0, \tag{16}$$

which gives, for $f_0 = M(v)$,

$$1+\frac{1}{k^2}\left[1+\frac{z+i\nu/k+i\nu k}{\sqrt{2}} Z\left(\frac{z+i\nu/k}{\sqrt{2}}\right)\right]=0. \tag{17}$$

Equations (15) and (17) can be solved numerically by standard techniques. For $k=0.5$, ω and γ are shown in Table I for the collisionless case and for three different values of ν, for which we have followed the time evolution of the system up to 35 plasma periods. In all cases, the initial condition is

$$g(x,v) = f_0(v)(1+\varepsilon \cos kx) \tag{18}$$

with $f_0(v) = M(v)$. In Fig. 2 we show the amplitude of the fundamental mode of the electric field (i.e., $|E_1|$, if the electric field is expanded according to $E(x,t) = \sum_k E_k(t) \exp(ikx)$) as a function of time in logarithmic scale for the cases $\nu = 0.01, 0.05, 0.1$ with $\varepsilon = 0.005$. The harmonics remain much smaller, as typical of all Vlasov simulations with periodic boundary conditions [2, 4, 5]. The damping rates resulting from the numerical simulations are $\gamma = 0.16$,

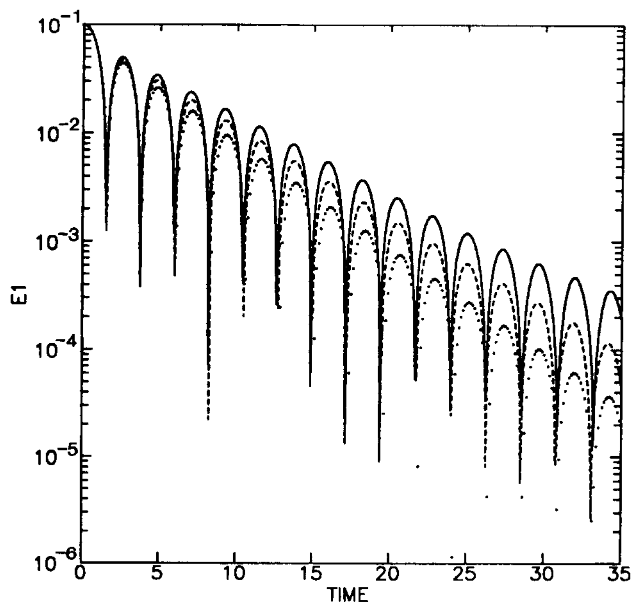

FIG. 2. $|E_1(t)|$ in logarithmic scale, $0 \leqslant t \leqslant 35$, for the Maxwellian case with $k=0.5$ and $\nu=0.01$ (solid line), $\nu=0.05$ (dashed line), and $\nu=0.1$ (dotted line).

0.19, 0.23, respectively, in good agreement with linear theory.

In a different case, with $k = 0.3$ and $\nu = 0.1$, we also present the level curves of the distribution function at selected times (Figs. 3a–d). As typical of Vlasov solutions [5], two vortices have formed in phase space, centered at $\pm v_\phi = \pm\omega/k \approx 3.866$ (as given by (14)) and travelling parallel to the space axis with velocities $\pm v_\phi$. Collisions, however, by drawing the distribution towards the Maxwellian, oppose the formation of such vortices, until they disappear between $t = 25$ and $t = 50$. Asymptotically, the distribution tends to a spatially uniform Maxwellian.

c. *Effect of Collisions on Linear Instabilities*

The linear dispersion relation again has the form (16), now with f_0 being different from the Maxwellian. For the symmetric bump-on-tail distribution (13), the dispersion relation (16) becomes

$$1 + \frac{1}{k^2}\left\{n_p\left[1 + \frac{z + i\nu k/n_p}{\sqrt{2}} Z\left(\frac{z}{\sqrt{2}}\right)\right] + \frac{n_b}{v_t}\left[2 + \frac{z_-}{\sqrt{2}} Z\left(\frac{z_-}{\sqrt{2}}\right) + \frac{z_+}{\sqrt{2}} Z\left(\frac{z_+}{\sqrt{2}}\right)\right]\right\} = 0,$$

where $z_\pm = (z \pm V_0)/v_t$, which, again, can be solved numerically by standard techniques. Table II shows ω and γ for the collisionless case and for three values of ν and $k = 0.3$. Note that the effect of the BGK collision operator, both for the Maxwellian and for the bump-on-tail case, is essentially in

TABLE II

Solution of the Dispersion Relation for the Bump-on-Tail Case with $k = 0.3$

ν	ω	γ
0.0	1.05	0.148
0.05	1.05	0.098
0.1	1.05	0.048
0.15	1.05	−0.002

a shift, by an amount equal to ν, of the imaginary part of the eigenvalue.

In the collisionless case, the unstable mode grows exponentially, with the growth rate predicted by the linear dispersion relation, until it saturates at some amplitude Γ because of particle trapping; after saturation, the electric field amplitude undergoes oscillations at the trapping frequency (much smaller than the plasma frequency), $\omega_b = \sqrt{k\Gamma}$, these oscillations being damped asymptotically [3, 4, 5, 15]. Collisions, by drawing the distribution toward a spatially uniform Maxwellian, tend to oppose the instability and to detrap particles. In Figs. 4 we show $|E_1|(t)$ in logarithmic scale for $\nu = 0.01$ and in Fig. 5 for $\nu = 0.05$, 0.1, and 0.15 with initial condition (18) and $f_0(v)$ given by (13). Here, $k = 0.3$ and $\varepsilon = 0.04$. In the collisionless case, the saturation amplitude is $\Gamma \approx 0.6$ which gives $\omega_b \approx 0.4$ [5]. The first value of ν is much smaller than the collisionless growth rate and the trapping frequency. As is seen in Fig. 4, the unstable mode grows according to the

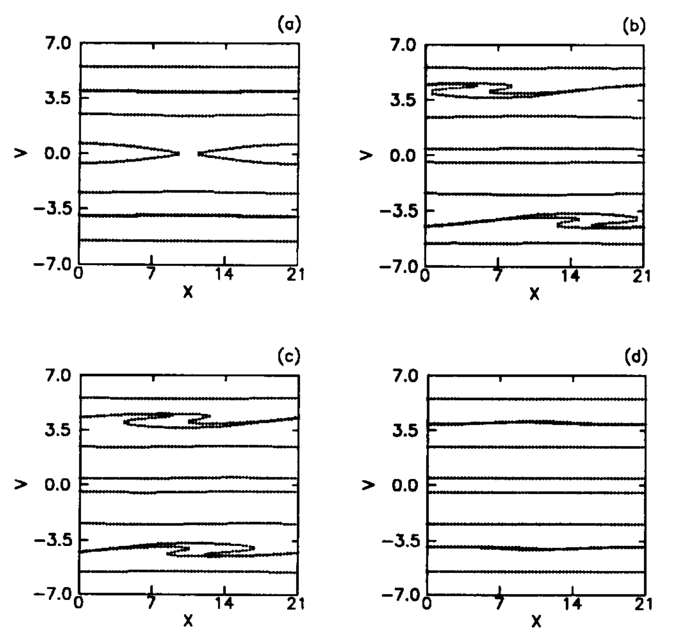

FIG. 3. (a)–(d) Level curves of $f(x, v, t)$ at $t = 0$ (a); $t = 25$ (b); $t = 26$ (c); $t = 50$ (d), for the Maxwellian case with $k = 0.3$ and $\nu = 0.1$.

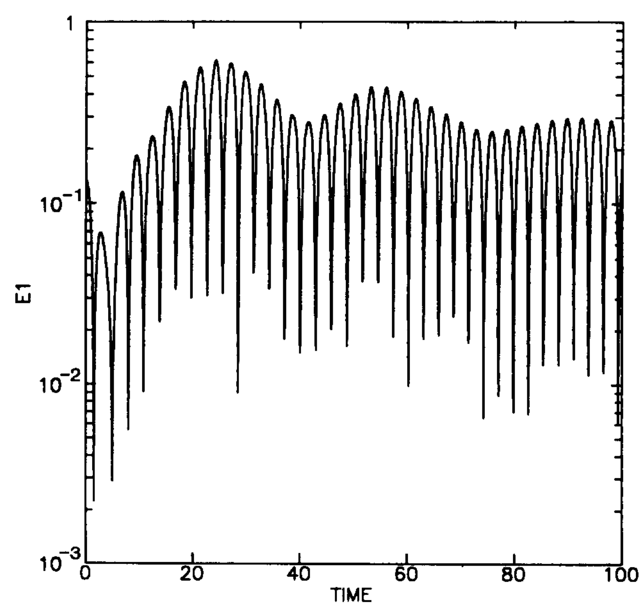

FIG. 4. $|E_1(t)|$ in logarithmic scale, $0 \leqslant t \leqslant 100$, for the bump-on-tail case with $k = 0.3$ and $\nu = 0.01$.

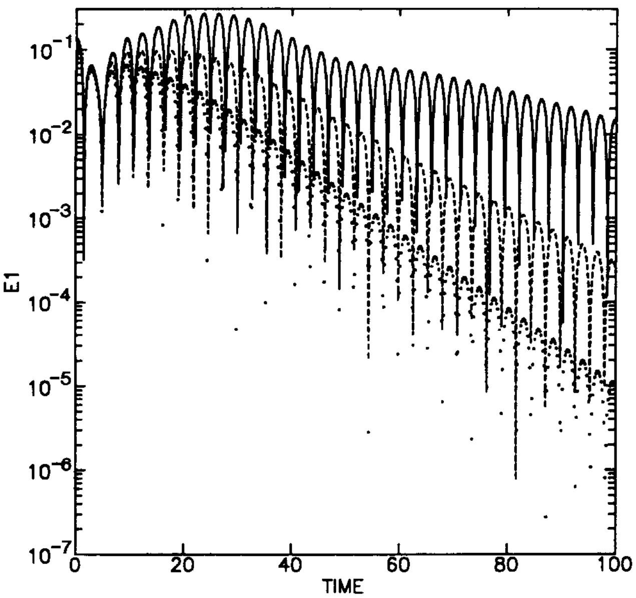

FIG. 5. $|E_1(t)|$ in logarithmic scale, $0 \leqslant t \leqslant 100$, for the bump-on-tail case with $k = 0.3$ and $v = 0.05$ (solid line), $v = 0.1$ (dashed line) and $v = 0.15$ (dotted line).

collisionless model until saturation and the onset of the oscillations at the trapping frequency occur. Just after the first of these latter oscillations, however, enough particles have been detrapped and the oscillations are destroyed. In the other three cases (Fig. 5) the growth rates are $\gamma = 0.097$, 0.047, -0.001, respectively, in agreement with linear theory. A remnant of the oscillations at the trapping frequency is present in the case with $v = 0.05$, while they have disappeared in the other cases. In the last case the instability has been completely suppressed.

4. CONCLUSIONS

In this work we have generalized the splitting scheme algorithm, which solves the one-dimensional Vlasov–Poisson system with immobile ions, by including collisional effects using the BGK model. The new algorithm calculates the variation of the distribution function along the Vlasov characteristics; this leads to a system of algebraic equations for the unknown values of the distribution on the mesh points. The accuracy of the splitting scheme (second order in Δt) is preserved. As a test for the validity of the algorithm we offer a few examples, including the relaxation of a spatially uniform distribution and the effect of collisions on linearly stable (Landau damping) and linearly unstable distributions.

ACKNOWLEDGMENTS

The author wishes to thank Professor P. F. Zweifel for many useful discussions. The people of the administrative and technical staff of the Pittsburgh Supercomputing Center are gratefully acknowledged for their helpful and competent assistance. This work was supported by the Center for Transport Theory and Mathematical Physics at the Virginia Polytechnic Institute and State University through NSF Grant DMS8922002 and by a financial support from GNFM (Gruppo Nazionale per la Fisica Matematica, Italy).

REFERENCES

1. C. G. Cheng and G. Knorr, *J. Comput. Phys.* **22**, 330 (1976).
2. M. Shoucri and R. Gagne', *Phys. Fluids* **21**, 1168 (1978).
3. M. Shoucri, *Phys. Fluids* **22**, 2038 (1979).
4. A. J. Klimas, *J. Comput. Phys.* **50**, 270 (1983).
5. L. Demeio and P. F. Zweifel, *Phys. Fluids B* **2**, 1252 (1990).
6. A. Simon and M. N. Rosenbluth, *Phys. Fluids* **19**, 1567 (1976).
7. C. Burnap, M. Miklavcic, B. W. Willis, and P. F. Zweifel, *Phys. Fluids* **28**, 110 (1985).
8. J. D. Crawford, "Hopf Bifurcation and Plasma Instabilities," Thesis, University of California, Berkeley, CA, 1983 (unpublished).
9. J. D. Crawford, *Contemp. Math.* **28**, 377 (1984).
10. P. L. Bhatnagar, E. P. Gross, and M. Krook, *Phys. Rev.* **94**, 511 (1954).
11. C. Cercignani, *Il Nuovo Cimento A* **87**, 96 (1985).
12. F. G. Cheremisin, *USSR Comput. Math. and Math. Phys.* **25**, 156 (1985).
13. Y. Sone, K. Aoki, and I. Yamashita, in *Proceedings, 15th International Symposium on Rarefield Gad Dynamics, Grado, Italy, 1986*, edited by V. Boffi and C. Cercignani (Teubner, Stuttgart, 1986).
14. A. Ghizzo, B. Izrar, P. Bertrand, E. Fijakow, M. R. Feix, and M. Shoucri, *Phys. Fluids* **31**, 72 (1988).
15. L. Demeio, "Nonlinear Evolution of Vlasov Equilibria," Thesis, Virginia Polytechnic Institute and State University, Blacksburg, VA, 1989 (unpublished).
16. A. J. Klimas, *J. Comput. Phys.* **68**, 202 (1987).
17. L. D. Landau, *J. Phys.* **10**, 25 (1956).
18. M. D. Arthur, W. Greenberg, and P. F. Zweifel, *Phys. Fluids* **20**, 1926 (1977).
19. B. D. Fried and S. D. Conte, *The Plasma Dispersion Function* (Academic Press, New York, 1961).